

Complex dynamics in coevolution models with ratio-dependent functional response

Per Arne Rikvold

*Center for Materials Research and Technology,
National High Magnetic Field Laboratory, and Department of Physics,
Florida State University, Tallahassee, Florida 32306-4350, USA
Tel.: +1-850-644-6814, Fax.: +1-850-644-6504, E-mail: prikvold@fsu.edu*

Abstract

We explore the complex dynamical behavior of two simple predator-prey models of biological coevolution that on the ecological level account for interspecific and intraspecific competition, as well as adaptive foraging behavior. The underlying individual-based population dynamics are based on a ratio-dependent functional response [W.M. Getz, *J. theor. Biol.* **108**, 623 (1984)]. Analytical results for fixed-point population sizes in some simple communities are derived and discussed. In long kinetic Monte Carlo simulations we find quite robust, approximate $1/f$ noise in species diversity and population sizes, as well as power-law distributions for the lifetimes of individual species and the durations of periods of relative evolutionary stasis. Adaptive foraging enhances coexistence of species and produces a metastable low-diversity phase and a stable high-diversity phase.

Keywords: Complex dynamics; Biological evolution; Coevolution; Predator-prey model; Functional response

I. INTRODUCTION

In recent years, there has been a growing recognition that processes at the ecological and evolutionary scales can be strongly linked [8, 44, 45, 48]. As a consequence, several approaches have been proposed, which model the complex process of coevolution in a fitness landscape that changes with the composition of the community, while spanning wide ranges of both temporal and taxonomic scales. Early steps in this direction were simulations of parapatric and sympatric speciation [6] and the coupled NK model with population dynamics [18, 19]. More recent contributions include the webworld model [2, 8, 9, 31, 32], the simple origination/extinction model of Nunes Amaral and Meyer [28], the speciation model of Rossberg et al. [39], the matching model of Rossberg et al. [40], the family of models introduced by Yoshida [47], the individual-based tangled-nature model [5, 7, 17] and simplified versions of the latter [34, 35, 37, 38, 41, 49], as well as network models [3, 4, 30]. Recently, large individual-based simulations have also been performed of parapatric and sympatric speciation [13, 14] and of adaptive radiation [15].

Many of the models mentioned above are deliberately simple, aiming to elucidate *universal* features that are largely independent of the finer details of the ecological interactions and the evolutionary mechanisms. While valuable from this point of view, the departure of many such models from mechanisms usually included in models of population dynamics and evolution has limited their acceptance in the biological community. A case in point are the tangled-nature model [5, 7, 17] and its simplifications [34, 35, 37, 38, 41, 49]. Here, we therefore introduce a modification of the latter, in which intra- and interspecific competition and adaptive foraging are introduced through ratio-dependent functional response functions.

Our motivation for this study is primarily a desire to understand the extent to which the long-time dynamics of complex coevolution models depend on details of the population dynamics. By using individual-based models with mutations, we avoid introducing the artificial separation between speciations and population dynamics inherent in all species-level models, including those mentioned above [2, 8, 9, 28, 31, 32, 39, 40, 47]. Despite being individual-based, our models enable fast simulation of large communities over time scales of tens of millions of generations. An important question that one would like to answer in the future is whether the avalanche-like mass extinctions observed in the fossil record are due to intrinsic fluctuations of the nonlinear dynamics [so-called self-organized criticality or SOC [26]], or to external perturbations such as asteroid impacts, volcanic eruptions, or climate changes, or to a combination of intrinsic and extrinsic causes [27]. In order to successfully address this question, it is necessary to understand better the influence that the population dynamics have on the intrinsic fluctuations in well-defined model systems. We find that the dynamics of the functional-response models studied in this paper differ from the tangled-nature type models studied earlier and also from each other, depending on whether or not adaptive foraging is implemented.

The remainder of this paper is organized as follows. The model without adaptive foraging is defined in Sec. II. For this model, analytical results for simple communities are derived and discussed in Sec. III, and kinetic Monte Carlo simulations of multispecies communities with mutations are performed and analyzed in Sec. IV. Adaptive foraging is introduced and investigated in Sec. V, both by numerical solution of the steady-state equations for two-species communities, and by long-time kinetic Monte Carlo simulations for evolving multispecies communities. A summary and conclusions are given in Sec. VI.

II. MODELS

We recently performed detailed analytical and simulational studies of the long-time dynamics and community structures of simplified tangled-nature models [34, 35, 37, 38, 41, 49]. In particular, the behaviors of mutualistic and predator-prey versions were compared by Rikvold [35], and community structures of the latter were compared with data from real ecosystems by Rikvold and Sevim [37]. Here we first describe features of these models that are shared by the new models that will be introduced below. More detailed descriptions of our previous models are given by Rikvold [35] and Rikvold and Sevim [37].

A. Shared features

The mechanism for selection between several interacting species is provided by the reproduction rates in an individual-based population dynamics with nonoverlapping generations. At the end of each generation, each individual of species I reproduces asexually, giving birth to a fixed number F of offspring with probability P_I before dying, or it dies without offspring with probability $(1 - P_I)$. Each P_I depends on the set $\{n_J(t)\}$ of population sizes of all the species resident in the community in generation t through interspecies interactions and other model parameters as described below. The interactions are determined by the random *interaction matrix* \mathbf{M} [43], which is constructed at the beginning of a simulation run, and thereafter kept constant. If M_{IJ} is positive and M_{JI} negative, then I is a predator and J its prey, and vice versa. If both matrix elements are positive, the relationship is a mutualistic one, while both negative indicate an antagonistic relationship.

The species are defined by a haploid, binary “genome” of length L , as in Eigen’s model for molecular evolution [10, 11], and the potential species are identified by the index $I \in [0, 2^L - 1]$. Typically, only $\mathcal{N}(t) \ll 2^L$ of these potential species are actually resident in the community at any one time t .

New species enter the community as each offspring organism may mutate with a small probability μ . Mutation consists in flipping a randomly chosen bit in the genome, and a mutated individual is assumed to belong to a different species than its parent, with different properties. Genotype and phenotype are thus in one-to-one correspondence in these models. This is a highly idealized picture, which is introduced to maximize the pool of different species available within the computational resources. The approximation is justified by a computational study, in which species differing by as many as $L/2$ bits have correlated properties [41]. Remarkably, it was shown that even strong correlations between the phenotypes of parents and offspring are relatively unimportant for the long-time dynamical properties.

Regardless of the functional form of P_I , the time development of the mean population sizes, $\langle n_I(t) \rangle$, is described by a set of coupled difference equations,

$$\begin{aligned} \langle n_I(t+1) \rangle &= \langle n_I(t) \rangle F P_I(\{\langle n_J(t) \rangle\}) [1 - \mu] \\ &\quad + (\mu/L) F \sum_{K(I)} \langle n_{K(I)}(t) \rangle P_{K(I)}(\{\langle n_J(t) \rangle\}), \end{aligned} \quad (1)$$

where $K(I)$ represents the L species that can be generated from I by a single mutation.

B. Simplified tangled-nature models

In these models, the reproduction probability for an individual of species I is given by the nonlinear function

$$P_I(t) = \frac{1}{1 + \exp[-\Delta_I(R, \{n_J(t)\})]}, \quad (2)$$

where R is an external resource that is renewed at the same level each generation. The function Δ_I is given by

$$\Delta_I(R, \{n_J(t)\}) = -b_I + \frac{\eta_I R}{N_{\text{tot}}(t)} + \sum_J \frac{M_{IJ} n_J(t)}{N_{\text{tot}}(t)} - \frac{N_{\text{tot}}(t)}{N_0}. \quad (3)$$

Here b_I is a “reproduction cost” (always positive), and η_I (positive for primary producers or autotrophs, and zero for consumers or heterotrophs) is the ability of individuals of species I to utilize the external resource R , while N_0 is an environmental carrying capacity [24] [a.k.a. Verhulst factor [46]]. The total population size is $N_{\text{tot}}(t) = \sum_J n_J(t)$.

Two versions of this model were studied in earlier work. In the first version there is no external resource or birth cost, and the off-diagonal elements of \mathbf{M} are stochastically independent and uniformly distributed over $[-1, +1]$, while the diagonal elements are zero. This model evolves toward mutualistic communities [1], in which all species are connected by asymmetric, mutually positive interactions [35, 38, 41, 49].

In the predator-prey version of the model, a small minority of the potential species (typically 5%) are primary producers, while the rest are consumers. The off-diagonal part of the interaction matrix is antisymmetric, with the additional restriction that a producer cannot also prey on a consumer [34, 35, 37]. In simulations we took b_I and the nonzero η_I as independent and uniformly distributed on $(0, +1]$. This model generates simple food webs with up to three trophic levels [34, 35, 37].

Both of these models provide interesting results, which include intermittent dynamics with power spectral densities (PSDs) of diversities and population sizes that exhibit approximate $1/f$ noise, as well as power-law distributions for the lifetimes of individual species and the duration of quiet periods of relative evolutionary stasis. From a theoretical point of view they also have the great advantage that the mean-field equation for the steady-state average population sizes, Eq. (1), in the absence of mutations reduces to a set of quadratic equations (linear if $N_0 = \infty$) and thus can easily be solved exactly [35, 37, 38, 49]. The models thus provide useful benchmarks for more realistic, but generally highly nonlinear models, like the ones defined below.

The population dynamics defined by Eqs. (2) and (3) have some less realistic features. In particular, by summing over positive and negative terms in Δ_I , the models enable species with little food to remain near a steady state if they are also not very popular as prey, or have very low birth cost. Another problem is the *ad-hoc* nature of the normalization by the total population size $N_{\text{tot}}(t)$ in the resource and interaction terms in Δ_I . While this is the source of the models’ analytic solvability, it implies an indiscriminate, universal competition without regard to whether or not two species directly utilize the same resources or share a common predator. The purpose of the present paper is to develop models with more realistic population dynamics and explore their complex dynamics on time scales from ecological (short) to evolutionary (long).

C. Functional-response model without adaptive foraging

Here we develop a model with population dynamics that include competition between different predators that prey on the same species, as well as intraspecific competition and a saturation effect expected to occur for a predator with abundant prey. In doing so, we retain from the models discussed above the important role of the interaction matrix \mathbf{M} , as well as the mutation process of the binary “genome” and the restriction to nonoverlapping generations.

We first deal with the competition between predator species by defining the number of individuals of J that are available as prey for I , corrected for competition from other predator species, as

$$\hat{n}_{IJ} = \frac{n_I M_{IJ}}{\sum_L^{\text{pred}(J)} n_L M_{LJ}} n_J, \quad (4)$$

where $\sum_L^{\text{pred}(J)}$ runs over all L such that $M_{LJ} > 0$, i.e., over all predators of J . Thus, $\sum_I^{\text{pred}(J)} \hat{n}_{IJ} = n_J$, and if I is the only predator consuming J , then $\hat{n}_{IJ} = n_J$.

Analogously, we define the competition-adjusted external resources available to a producer species I as

$$\hat{R}_I = \frac{n_I \eta_I}{\sum_L n_L \eta_L} R. \quad (5)$$

As in the case of predators, $\sum_I \hat{R}_I = R$, and a sole producer species has all of the external resources available to it: $\hat{R}_I = R$. With these definitions, the total, competition-adjusted resources available for the sustenance of species I are

$$\hat{S}_I = \eta_I \hat{R}_I + \sum_J^{\text{prey}(I)} M_{IJ} \hat{n}_{IJ}, \quad (6)$$

where $\sum_J^{\text{prey}(I)}$ runs over all J such that $M_{IJ} > 0$, i.e., over all prey of I , and $\eta_I = 0$ if I is a heterotroph.

A central concept of the model is the *functional response* of species I with respect to J , Φ_{IJ} [8, 21]. This is the rate at which an individual of species I consumes individuals of J . The simplest functional response corresponds to the Lotka-Volterra model [24]: $\Phi_{IJ} = n_J$ if $M_{IJ} > 0$ and 0 otherwise. However, it is reasonable to expect that the consumption rate should saturate in the presence of very abundant prey [21]. For ecosystems consisting of a single pair of predator and prey, or a simple chain reaching from a bottom-level producer through intermediate species to a top predator, the most common forms of functional response are due to Holling [21]. For more complicated, interconnected food webs, a number of functional forms have been proposed in the recent literature [8, 9, 22, 23, 31, 32, 42], but there is as yet no agreement about a standard form. Here we choose the ratio-dependent [8, 9, 12, 31, 32, 33] Holling Type II form [21], originally introduced by Getz [16],

$$\Phi_{IJ} = \frac{M_{IJ} \hat{n}_{IJ}}{\lambda \hat{S}_I + n_I}, \quad (7)$$

where $\lambda \in (0, 1]$ is the metabolic efficiency of converting prey biomass to predator offspring. The ratio dependence corresponds to intraspecific competition [16]. Analogously, the func-

tional response of a producer species I toward the external resource R is

$$\Phi_{IR} = \frac{\eta_I \hat{R}_I}{\lambda \hat{S}_I + n_I}. \quad (8)$$

In both cases, if $\lambda \hat{S}_I \ll n_I$, then the consumption rate equals the resource ($M_{IJ} \hat{n}_{IJ}$ or $\eta_I \hat{R}_I$) divided by the number of individuals of I , thus expressing intraspecific competition for scarce resources. In the opposite limit, $\lambda \hat{S}_I \gg n_I$, the consumption rate is proportional to the ratio of the specific, competition-adjusted resource to the competition-adjusted total available sustenance, \hat{S}_I . The total consumption rate for an individual of I is therefore

$$C_I = \Phi_{IR} + \sum_J^{\text{prey}(I)} \Phi_{IJ} = \frac{\hat{S}_I}{\lambda \hat{S}_I + n_I} = \begin{cases} \hat{S}_I/n_I & \text{for } \lambda \hat{S}_I \ll n_I \\ 1/\lambda & \text{for } \lambda \hat{S}_I \gg n_I \end{cases}.$$

The birth probability is assumed to be proportional to the consumption rate,

$$B_I = \lambda C_I \in [0, +1], \quad (9)$$

while the probability that an individual of I avoids death by predation until attempting to reproduce at the end of the generation is

$$A_I = 1 - \sum_J^{\text{pred}(I)} \Phi_{JI} \frac{n_J}{n_I}. \quad (10)$$

The total reproduction probability for an individual of species I in this model is thus

$$P_I(t) = A_I(t) B_I(t). \quad (11)$$

III. ANALYTICAL RESULTS

The functional-response model defined in Sec. IIC is much less amenable to analytic treatment than the models we have considered previously. In particular, the simultaneous set of equations,

$$FP_I(\{n_j^*\}) = 1 \quad (12)$$

where F is the fecundity, which defines the fixed-point solution $\{n_j^*\}$ of Eq. (1) for multispecies communities in the mutation-free limit, cannot be solved analytically in general. However, some special cases can be solved explicitly. Although these analytical solutions are highly model-specific, they provide useful insight into some of the simplest effects of interspecies interactions and intra- and interspecific competition.

A. Two competing producers with intraguild predation

Consider two producer species characterized by their coupling constants, η_1 and η_2 . In the noninteracting case, $M_{21} = M_{12} = 0$, the species are subject to competitive exclusion, so that only one species, the one with the maximum value of η_I , can survive with a nonzero fixed-point population, $n_{\max}^* = \lambda \eta_{\max} (F - 1) R$. The only exception is the degenerate case

of $\eta_1 = \eta_2$, in which the two species are dynamically indistinguishable. The property of competitive exclusion in the noninteracting limit is shared with the simplified tangled-nature models discussed previously, and it carries over to sets of any number of noninteracting producers [35].

For the interacting case, $M_{21} \in (0, 1]$ (and $M_{12} = -M_{21}$), which is a simple example of intraguild predation, the solution to Eq. (12) is

$$n_1^* = \frac{\eta_1 \lambda (F - 1) [\eta_1^2 (1 - M_{21}) - \eta_2^2 (1 - M_{21})]}{\eta_1 (1 - M_{21}) [\eta_1 + \eta_2 \lambda (F - 1) M_{21}] - \eta_2^2} R \quad (13)$$

and

$$n_2^* = \frac{\eta_1^3 \lambda^2 (F - 1)^2 (1 - M_{21})^2 M_{21}}{\eta_1 (1 - M_{21}) [\eta_1 + \eta_2 \lambda (F - 1) M_{21}] - \eta_2^2} R, \quad (14)$$

as long as both populations are nonnegative. This requires $0 \leq \eta_2 \leq \eta_1 \sqrt{1 - M_{21}}$. These rather complicated analytical solutions are best interpreted graphically as in Fig. 1(a), which shows the case $\lambda = 1$, $\eta_1 = 1$, and $M_{21} = 0.5$. Other parameter values give similar results. As η_2 is increased from zero, the population of species 2, n_2 , first decreases weakly as it competes directly for resources with species 1, which is its only source of support at $\eta_2 = 0$. Differentiation of the denominator in Eq. (14) shows that n_2 reaches its minimum at $\eta_2 = \eta_1 \lambda (1 - M) M / 2$. For larger η_2 it increases nonlinearly due to the term quadratic in η_2 in the denominator. The combined competition and predation from species 2 causes n_1 to decrease monotonically, first linearly in η_2 and later nonlinearly until it reaches zero at $\eta_2 = \eta_1 \sqrt{1 - M_{21}}$. For larger η_2 , species 2 completely excludes species 1, and the stationary solution is $n_2^* = \lambda \eta_2 (F - 1) R$ and $n_1^* = 0$, even though η_2 may still be less than η_1 . The two solutions for n_2 join continuously at $\eta_2 = \eta_1 \sqrt{1 - M_{21}}$, and there are no other attractive fixed points for the mutation-free dynamics. Looking at the total population size, $n_1 + n_2$, we find that it is a continuous, convex function of η_2 , with a shallow minimum at $\eta_2 = \eta_1 \left\{ 1 - \sqrt{1 - \lambda (F - 1) (1 - M)} \right\}$. (The solution $n_1^* = \lambda \eta_1 (F - 1) R$ and $n_2^* = 0$ is a fixed point as well, but it is repulsive under perturbations to n_2^* .)

B. \mathcal{N} -species food chain

The other case, for which the fixed-point population sizes can be found relatively easily, is a “food chain” in which species $I + 1$ feeds exclusively on the preceding one, I . The fixed-point equation (12) then takes the form

$$F \left(1 - \frac{M_{I+1} n_{I+1}^*}{\lambda M_{I+1} n_I^* + n_{I+1}^*} \right) \frac{\lambda M_I n_{I-1}^*}{\lambda M_I n_{I-1}^* + n_I^*} = 1, \quad (15)$$

where for simplicity we write M_I for $M_{I,I-1}$.

With boundary conditions $n_0^* = R$ and $n_\infty^* = 0$, and with all $M_I = M$ (we define $M_1 = \eta_1$), this set has a geometrically decreasing solution of the form $n_I^* = R \alpha^I$ with

$$\alpha = \frac{\lambda M}{2} \left\{ \sqrt{F [4M + F(1 - M)^2]} + F(1 - M) - 2 \right\} < 1. \quad (16)$$

This solution is included in Fig. 1(b) as the one corresponding to $\mathcal{N} = \infty$. [Parameter values for which $\alpha \geq 1$ (essentially very large fecundity F combined with M and λ near unity) are unrealistic.]

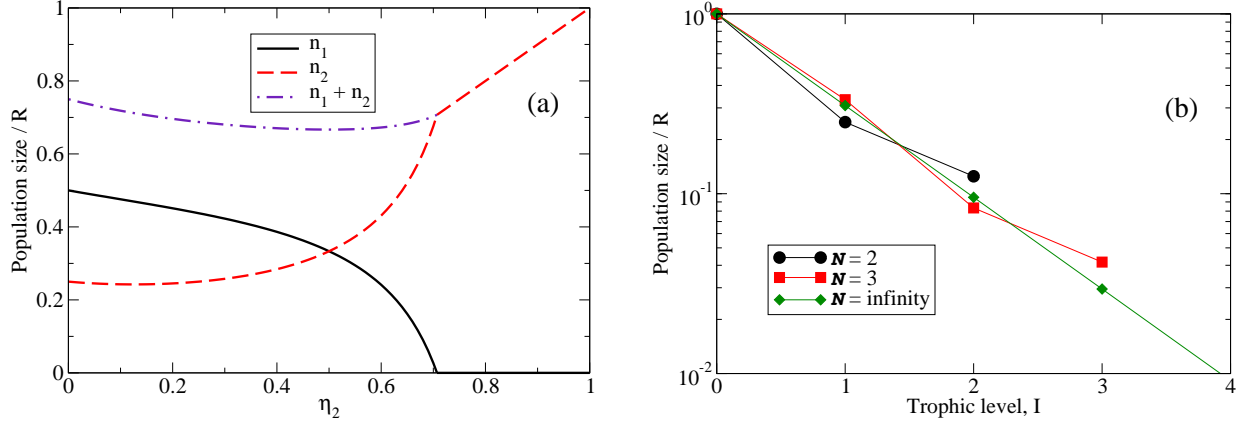


FIG. 1: **(a)** Population sizes for two competing producer species with intraguild predation in the functional-response model without adaptive foraging, shown as functions of η_2 . The other parameters are $\eta_1 = 1.0$, $M_{21} = 0.5$, and $\lambda = 1$. See the text for details. **(b)** Population sizes for food chains of \mathcal{N} species with $\lambda = 1$ and $M = 0.5$. See the text for details.

If it is instead known that there are \mathcal{N} trophic levels, so that $n_{\mathcal{N}+1}^* = 0$, then the fixed-point equations can be solved analytically in an iterative fashion as follows.

1. Solve the linear fixed-point equation (12) expressing $n_{\mathcal{N}}^* = \text{const.}$,

$$F \frac{\lambda M_{\mathcal{N}} n_{\mathcal{N}-1}^*}{\lambda M_{\mathcal{N}} n_{\mathcal{N}-1}^* + n_{\mathcal{N}}^*} = 1,$$

for $n_{\mathcal{N}-1}^*$.

2. Insert the solution for $n_{\mathcal{N}-1}^*$ in terms of $n_{\mathcal{N}}^*$ into the next equation in the hierarchy (the one expressing $n_{\mathcal{N}-1}^* = \text{const.}$),

$$F \left(1 - \frac{M_{\mathcal{N}} n_{\mathcal{N}}^*}{\lambda M_{\mathcal{N}} n_{\mathcal{N}-1}^* + n_{\mathcal{N}}^*} \right) \frac{\lambda M_{\mathcal{N}-1} n_{\mathcal{N}-2}^*}{\lambda M_{\mathcal{N}-1} n_{\mathcal{N}-2}^* + n_{\mathcal{N}-1}^*} = 1,$$

and cancel common factors to get a linear equation for $n_{\mathcal{N}-2}^*$ in terms of $n_{\mathcal{N}}^*$.

3. Continue until obtaining n_0^* in terms of $n_{\mathcal{N}}^*$.
4. Rescale the solutions to give $n_0^* = R$.

With large \mathcal{N} and I -independent M_I , this solution converges toward the decreasing geometric one presented above for $I \ll \mathcal{N}$, as shown in Fig. 1(b).

IV. NUMERICAL RESULTS FOR THE FUNCTIONAL-RESPONSE MODEL

We simulated the functional-response model defined in Sec. II C over $2^{24} = 16\,777\,216$ generations (plus 2^{20} generations “warm-up”) for the following parameters: genome length $L = 21$ ($2^{21} = 2\,097\,152$ potential species), external resource $R = 16\,000$, fecundity $F = 2$,

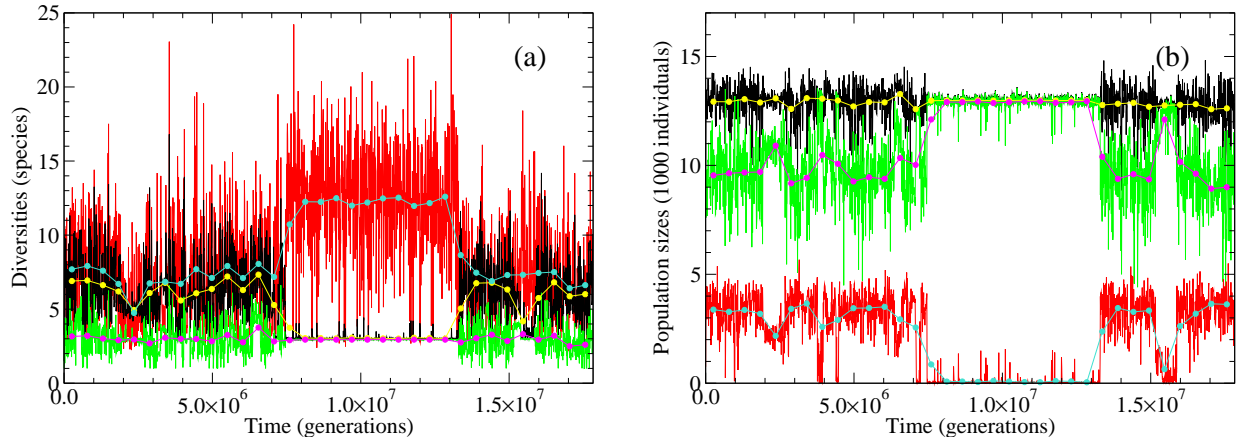


FIG. 2: Time series of diversities (a) and population sizes (b) for one specific simulation run of the functional-response model without adaptive foraging. The strongly fluctuating curves in the background are sampled every 8192 generations, while the smooth curves with data points in contrasting colors that are overlaid in the foreground are running averages over 524 288 generations. Black with light gray (yellow online) overlay: all species. Light gray with dark gray overlay (green and magenta online): producers. Dark gray with light gray overlay (red and cyan online): consumers.

mutation rate $\mu = 10^{-3}$, proportion of producers $c_{\text{prod}} = 0.05$, interaction matrix \mathbf{M} with connectance $C = 0.1$ and nonzero elements with a symmetric, triangular distribution over $[-1, +1]$, and $\lambda = 1.0$. (The high value of λ is of course biologically unrealistic, and it was chosen to obtain a larger population of heterotrophs for a computationally manageable autotroph population.) We ran five independent runs, each starting from 100 individuals of a single, randomly chosen producer species.

A. Time series

Time series of diversities (effective numbers of species) and population sizes for one realization are shown in Fig. 2. To filter out noise from low-population, unsuccessful mutations, we define the diversity as the exponential Shannon-Wiener index [20]. This is the exponential function of the information-theoretical entropy of the population distributions, $D(t) = \exp[S(\{n_I(t)\})]$, where $S(\{n_I(t)\}) = -\sum_{\{I|\rho_I(t)>0\}} \rho_I(t) \ln \rho_I(t)$ with $\rho_I(t) = n_I(t)/N_{\text{tot}}(t)$ for the case of all species, and analogously for the producers and consumers separately.

The time series for both diversities and population sizes display intermittent behavior with quiet periods of varying lengths, separated by brief periods of high evolutionary activity. The intermittency is highlighted by the time series for the accumulation of new and extinct species, shown in Fig. 3. In this respect, the results are similar to those seen for the simplified tangled-nature models in earlier work [34, 35, 38, 41]. However, diverse communities in this model are less stable than those produced by the simplified tangled-nature models. It is possible that this instability is related to the tendency of “triangles” consisting of two species competing for a common resource while one of them also feeds on the other one

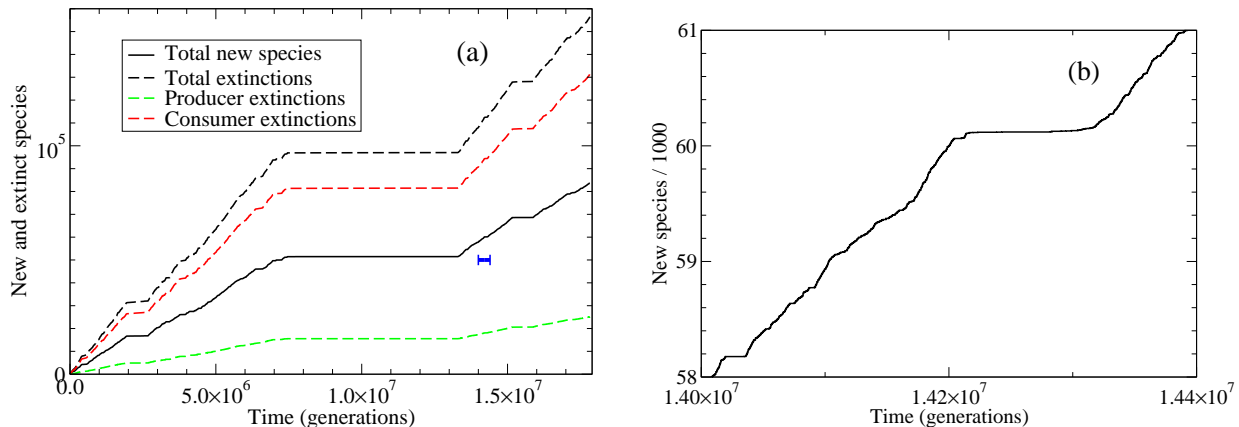


FIG. 3: **(a)** Time series of the accumulation of new and extinct species in the same simulation run depicted in Fig. 2. The solid, black curve shows the total number of different species that have at least once attained a population size $n_I > 1000$ by time t . The dashed curves count the total number of species that have gone extinct after attaining a maximum population greater than 1000. The black dashed curve refers to all species, the light gray one (green online) to producers, and the dark gray one (red online) to consumers. The ratio of approximately 1.89 between the dashed and full black curves indicate that major species recur on average about twice during the evolution. This is an artifact of the finite genome length. **(b)** The detailed, intermittent structure of new species (the solid, black curve in **(a)**) over 400 000 generations. The interval is indicated by the short, horizontal bar in **(a)**.

(intraguild predation) to collapse, that we discussed in Sec. III A. The instability expresses itself in a tendency for this model to flip randomly between an active phase with a diversity near ten, and a “garden of Eden” phase of one or a few producer species with a very low population size of numerous unstable consumer species, such as the one seen around 10 million generations in Figs. 2 and 3(a).

B. Power-spectral densities

To obtain information about the intensity of fluctuations in the evolving community, we calculate power-spectral densities, or PSDs.[50] These are presented in Fig. 4 for the diversities and the population sizes (Fig. 4(a)) and the intensity of extinction events (Fig. 4(b)). The former two are shown for the total population, as well as separately for the producers and consumers. All three are similar. Extinction events are recorded as the number of species that have attained a population size greater than one, which go extinct in generation t (marked as “Species” in the figure), while extinction sizes are calculated by adding the maximum population sizes attained by all species that go extinct in generation t (marked as “Population” in the figure). The PSDs for all the quantities shown exhibit approximate $1/f$ behavior. For the diversities and population sizes, this power law extends over more than five decades in time. The extinction measures, on the other hand, have a large background of white noise for frequencies above 10^{-3} generations $^{-1}$, probably due to the high rate of extinction of unsuccessful mutants. For lower frequencies, however, the behavior is consis-

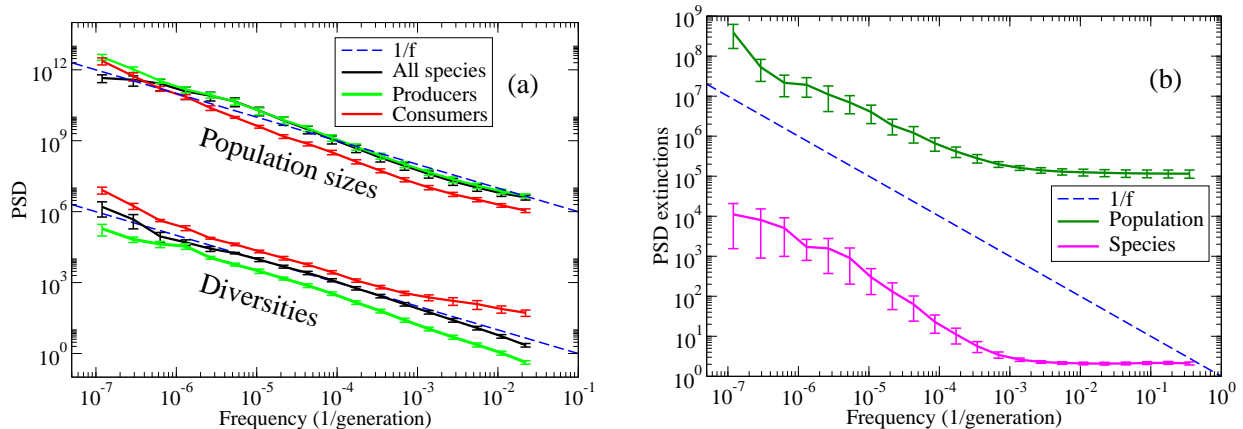


FIG. 4: **(a)** PSDs for the diversities and population sizes, each recorded separately for all species and for producers and consumers. The time series were sampled every 16 generations. **(b)** PSDs for the extinction activity, sampled every generation. In both parts of the figure, the results are averaged over five independent simulation runs. See discussion in the text.

tent with $1/f$ noise within the limited accuracy of our results. We note that the apparent $1/f$ behavior in the PSD of extinction events in the model of Nunes Amaral and Meyer [28] extends over only one decade in frequency.

C. Species lifetimes and durations of quiet periods

The evolutionary dynamics can also be characterized by histograms of characteristic time intervals, such as the time from emergence till extinction of a species (species lifetimes) or the time intervals during which some indicator of evolutionary activity remains continuously below a chosen cutoff (duration of evolutionarily quiet periods). Histograms of species lifetimes are shown in Fig. 5(a). As our indicator of evolutionary activity we use the magnitude of the logarithmic derivative of the diversity, $|dS/dt|$, and histograms for the resulting durations of quiet periods, calculated with different cutoffs, are shown in Fig. 5(b). Both quantities display approximate power-law behavior with an exponent near -2 , consistent with the $1/f$ behavior observed in the PSDs [29, 38]. It is interesting to note that the distributions for these two quantities for this model have approximately the same exponent. This is consistent with the previously studied, mutualistic model [34, 35, 38], but not with the predator-prey model [34, 35, 37]. We believe the linking of the power laws for the species lifetimes and the duration of quiet periods indicate that the communities formed by the present model are relatively fragile, so that all member species tend to go extinct together in an avalanche-like “mass extinction.” In contrast, the previously studied predator-prey model produces simple food webs that are much more resilient against the loss of a few species, and as a result the distribution of quiet-period durations decays with an exponent near -1 [34, 35, 37].

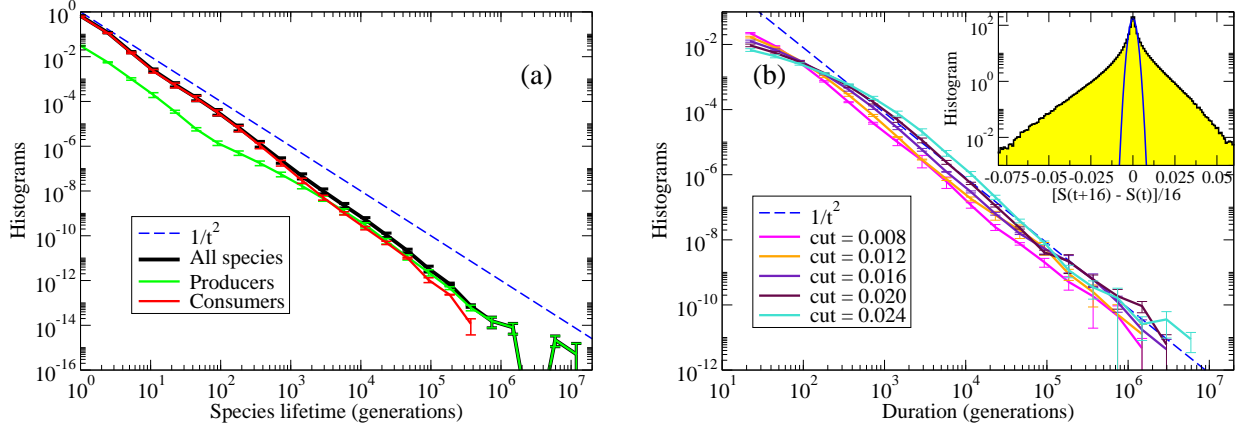


FIG. 5: **(a)** Histograms of species lifetimes, shown for all species, as well as separately for producers and consumers. **(b)** Histograms of the durations of evolutionarily quiet periods, defined as the times that the logarithmic derivative of the diversity, $|dS/dt|$ (averaged over 16 generations), falls continuously below some cutoff. The inset is a histogram of dS/dt , showing a Gaussian center with approximately exponential wings. The parabola in the foreground is a Gaussian fit to this central peak. The cutoff values for the main figure, between 0.008 and 0.024, were chosen on the basis of this distribution. The data in both parts of the figure are averaged over five independent simulation runs, and the error bars represent standard errors based on the differences between runs.

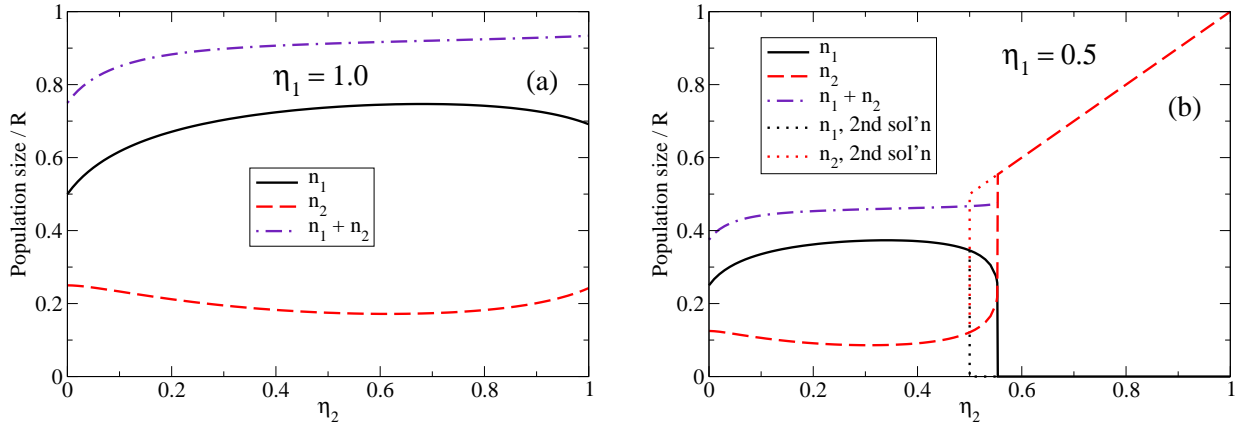


FIG. 6: Population sizes for two competing producer species with intraguild predation in the model with adaptive foraging, shown as functions of η_2 . **(a)** $\eta_1 = 1.0$. **(b)** $\eta_1 = 0.5$. In both cases, $\lambda = 1$ and $M_{21} = 0.5$. See further discussion in the text.

V. MODEL WITH ADAPTIVE FORAGING

The model studied above is one in which species forage indiscriminately over all available resources, with the output only limited by competition. Also, there is an implication that an individual's total foraging effort increases proportionally with the number of species to which it is connected by a positive M_{IJ} . A more realistic picture would be that an individual's

total foraging effort is constant and can either be divided equally, or concentrated on richer resources. The latter constitutes adaptive foraging. While one can go to considerable length devising optimal foraging strategies [8, 9, 31, 32], we here only use a simple scheme, in which individuals of I show a preference for prey species J , based on the interactions and population sizes (uncorrected for interspecific competition). The proportion of its foraging effort that I allots to J is approximated as

$$p_{IJ} = \frac{M_{IJ}n_J}{\eta_I R + \sum_K^{\text{prey}(I)} M_{IK}n_K}, \quad (17)$$

and analogously for the effort assigned to the external resource,

$$p_{IR} = \frac{\eta_I R}{\eta_I R + \sum_K^{\text{prey}(I)} M_{IK}n_K}. \quad (18)$$

The total foraging effort is thus normalized: $p_{IR} + \sum_J^{\text{prey}(I)} p_{IJ} = 1$. These preference factors are used to modify the reproduction probabilities by replacing all occurrences of M_{IJ} by $M_{IJ}p_{IJ}$ and of η_I by $\eta_I p_{IR}$ in Eqs. (4–8).

The adaptive foraging obviously has no effect on a simple food chain since no species in this case has more than one choice of prey. The analytical results thus remain as discussed in Sec. III B.

For the case of two competing producers with intraguild predation we did not obtain analytical results for the fixed-point population sizes, except for the special cases of $\eta_2 = 0$, which corresponds to a two-species food chain, and of $M_{21} = 0$, which reduces to simple competitive exclusion of the species with the lower η_I . However, numerical results for $M_{21} = 0.5$, obtained by iteration of Eq. (1) with $\mu = 0$, are given in Fig. 6. The results are similar for other values of the model parameters. The parameters in Fig. 6(a) are the same as in Fig. 1(a), and we see that the regime of two-species coexistence is significantly extended by the adaptive foraging and here covers the full range of η_2 . We also see that while n_2^* is reduced, compared to the case without adaptive foraging, both n_1^* and the total population, $n_1^* + n_2^*$, are significantly increased, indicating a more efficient overall resource utilization by the community. In Fig. 6(b) we reduce η_1 to 0.5 to explore the possibility that $\eta_2 > \eta_1$. We find that the coexistence solution extends up to $\eta_2 \approx 0.553$, where $n_1^* = n_2^*$ and the solution changes discontinuously to the familiar $n_2^* = \lambda(F - 1)\eta_2 R$ and $n_1^* = 0$. In fact, for η_2 between $\eta_1 = 0.5$ and 0.553, *both* solutions are locally stable under small perturbations. This is indicated by the dotted lines in the figure. Outside this range, the solutions shown are globally stable attractors. As in the case without adaptive foraging, the solution $n_1^* = \lambda\eta_1(F - 1)R$ and $n_2^* = 0$ is repulsive under perturbations to n_2^* .

The results of implementing the adaptive foraging strategy in long-time simulations of evolving multispecies communities are quite striking. The system now has a metastable low-diversity phase similar to the active phase of the non-adaptive model, from which it switches at a random time to a stable high-diversity phase with much smaller fluctuations. As seen in Fig. 7, the switchover is quite abrupt, and Fig. 8 shows that it is accompanied by a sudden reduction in the rate of emergence of new species. The existence of a stable high-diversity phase with increased producer and total populations and reduced consumer population in the case of adaptive foraging is consistent with the extension of the stability of two-species coexistence discussed above. The increased total population is consistent with the improved resource utilization, and the sudden nature of the transition from low to high diversity is

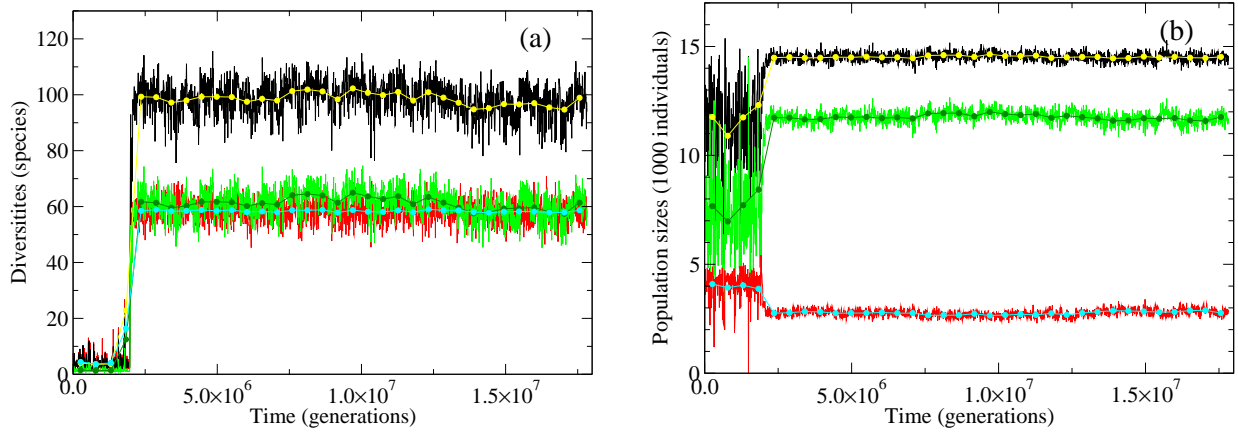


FIG. 7: Time series of diversities **(a)** and population sizes **(b)** for the model with adaptive foraging. The interpretation of the colors and lines are the same as in Fig. 2.

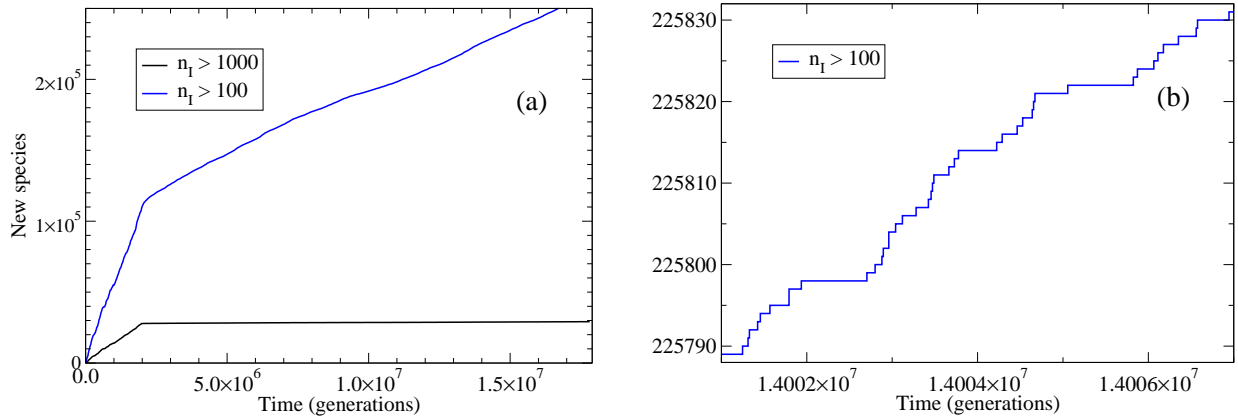


FIG. 8: **(a)** Time series of the number of new species that have reached a population greater than 1000 (lower curve) and greater than 100 (upper curve) in the same simulation run depicted in Fig. 7. **(b)** The detailed, intermittent structure of the upper curve in **(a)** on a very fine scale of 6000 generations. See discussion in the text.

consistent with the discontinuity and bistability, all observed in the adaptive two-species case. As adaptive foraging implies an effective reduction of omnivory, our results present a scenario in which reduced omnivory leads to increased community stability [25].

As seen in Fig. 9, the PSDs for both the diversities and population sizes in both phases show approximate $1/f$ noise for frequencies above 10^{-5} generations⁻¹. For lower frequencies, the metastable phase shows no discernible frequency dependence, while for the stable phase, the frequency dependence continues at least another decade. It thus appears that long-time correlations are not seen beyond about 10^5 generations in the metastable phase.

In fact, the system can also escape from the low-diversity phase to total extinction, which is an absorbing state, and in some of our simulation runs we avoided this by limiting $|M_{IJ}|$

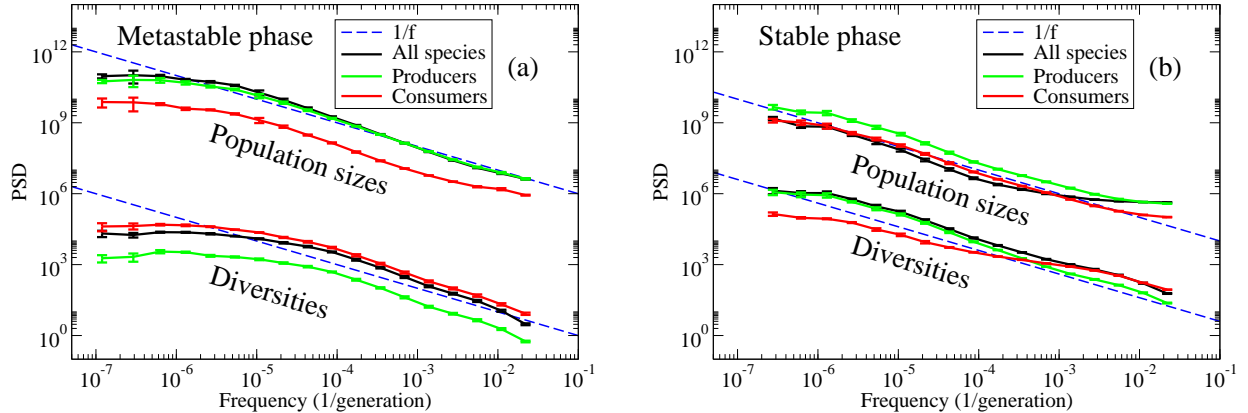


FIG. 9: PSDs for the diversities and population sizes in the metastable phase (averaged over three independent runs) **(a)**, and the stable phase (averaged over five independent runs) **(b)** for the model with adaptive foraging. Both show approximate $1/f$ noise for frequencies above about 10^{-5} . However, in the metastable phase the PSDs appear to approach constant levels for the lowest frequencies, indicating the absence of long-time correlations.

to less than 0.9. This restriction does not seem to have any effect on the dynamics in the high-diversity phase.

VI. CONCLUSIONS

In this paper we have extended our study of the long-time dynamics of a class of individual-based models with stochastic population dynamics, nonoverlapping generations, and random mutations during reproduction. Previous studies concentrated on simplified versions of the tangled-nature model [5, 7, 17], sharing with that model a reproduction probability defined by Eqs. (2) and (3) [34, 35, 37, 38, 41, 49]. While these models in the absence of mutations allow for exact, analytical solutions for the fixed-point populations of any given community of species, this convenient mathematical property is due to two somewhat unrealistic features. (i) The lumping together of resources and predation as respectively positive and negative contributions to the quantity Δ_I in Eq. (3). (ii) The normalization of the population sizes n_J in Δ_I by the total population size N_{tot} , which can be seen as an indiscriminate, universal competition effect.

Here, we therefore introduce population dynamics based on a functional response for predators versus their prey and for autotrophs versus the external resource. Interspecific competition is introduced through the competition-adjusted resources defined in Eq. (6), and intraspecific competition is accounted for by the ratio-dependent functional response due to Getz [16], Eq. (7). The probability for a live individual to give birth is given by Eq. (9), and the probability that an individual avoids being eaten before it can reproduce is given by Eq. (10). Their product, Eq. (11), is the total reproduction probability P_I .

We considered two versions of this model, one without adaptive foraging, and one with it. While a complete analytic solution of the fixed-point communities is not feasible for either model, we obtained solutions for a simple food chain of predators supplied by a single producer species. For the model without adaptive foraging we also obtained an analytic

solution for the coexistence of two producer species, one of which also acts as a predator toward the other (intraguild predation). A corresponding analytic solution was not found for the model with adaptive foraging. However, numerical solutions of Eq. (1) with $\mu = 0$ showed a significantly expanded parameter range for coexistence, including a regime where both coexistence and competitive exclusion are locally attractive fixed-point solutions. The coexistence solution also exhibited a decrease in the predator population, which was more than compensated by an increase in the prey population, leading to a significant increase in the total population size; in other words to a more efficient resource exploitation by the overall community.

Long-time kinetic Monte Carlo simulations of the two models produced time series of diversities and population sizes that exhibit approximate $1/f$ noise in a wide frequency range. However, there are significant differences between the models.

Without adaptive foraging, the community flips randomly back and forth between an evolutionarily active phase with diversities around ten, and another phase with a very low evolutionary turnover, a small number of coexisting producer species, and a very small population of unsuccessful consumers.

With adaptive foraging, the model displays a metastable phase which resembles the active phase in the previous case. After a random amount of time, this phase suddenly gives way, either to total extinction, or to a new, stable phase with an order of magnitude larger diversities and somewhat higher total population size. The relative fluctuations in this phase are much smaller than in the other phases in either model. We find it reasonable to believe that the increased diversity and population size in the stable phase of the model with adaptive foraging are related to the increased tendency toward species coexistence in this model, observed in Fig. 6. This stabilization of the communities is consistent with observations for the web-world model with adaptive foraging [8, 9, 31, 32]. The dynamics and community structures of the stable phase in the model with adaptive foraging are studied in detail in a forthcoming paper [36].

In summary, the models studied here show that some aspects of the long-time dynamics, such as the $1/f$ noise in diversities, population sizes, and extinction sizes, are quite robust. However, the community structures and their stability or lack thereof show significant differences, both from previously studied tangled-nature type models, and depending on whether or not adaptive foraging is implemented. A comprehensive understanding of the universal and nonuniversal fluctuation properties of large-scale coevolution and their relation to avalanches of species extinctions is likely to demand a combination of implementations of more realistic population dynamics and mutation mechanisms, and further study of minimalistic models.

Acknowledgments

Supported in part by U.S. National Science Foundation Grant Nos. DMR-0444051 and DMR-0802288.

-
- [1] Bascompte, J., Jordano, P., Olesen, J. M., 2006. Asymmetric coevolutionary networks facilitate biodiversity maintenance. *Science* 312, 431–433.

- [2] Caldarelli, G., Higgs, P. G., McKane, A. J., 1998. Modelling coevolution in multispecies communities. *J. theor. Biol.* 193, 345–358.
- [3] Chowdhury, D., Stauffer, D., 2005. Evolutionary ecology in-silico: Does mathematical modelling help in understanding the generic trends? *J. Biosciences* 30, 277–287.
- [4] Chowdhury, D., Stauffer, D., Kunwar, A., 2003. Unification of small and large time scales for biological evolution: Deviations from power law. *Phys. Rev. Lett.* 90, 068101.
- [5] Christensen, K., di Collobiano, S. A., Hall, M., Jensen, H. J., 2002. Tangled-nature: A model of evolutionary ecology. *J. theor. Biol.* 216, 73–84.
- [6] Crosby, J. L., 1970. The evolution of genetic discontinuity: Computer models of the selection of barriers to interbreeding between subspecies. *Heredity* 25, 253–297.
- [7] di Collobiano, S. A., Christensen, K., Jensen, H. J., 2003. The tangled nature model as an evolving quasi-species model. *J. Phys. A* 36, 883–891.
- [8] Drossel, B., Higgs, P. G., McKane, A. J., 2001. The influence of predator-prey population dynamics on the long-term evolution of food web structure. *J. theor. Biol.* 208, 91–107.
- [9] Drossel, B., McKane, A., Quince, C., 2004. The impact of non-linear functional responses on the long-term evolution of food web structure. *J. theor. Biol.* 229, 539–548.
- [10] Eigen, M., 1971. Selforganization of matter and evolution of biological macromolecules. *Naturwissenschaften* 58, 465.
- [11] Eigen, M., McCaskill, J., Schuster, P., 1988. Molecular quasi-species. *J. Phys. Chem.* 92, 6881–6891.
- [12] Filotas, E., Grant, M., Parrott, L., Rikvold, P. A., 2008. Community-driven dispersal in an individual-based predator-prey model. *Ecol. Complex.* 5, 238–251.
- [13] Gavrillets, S., Boake, C. R. B., 1998. On the evolution of premating isolation after a founder event. *Am. Nat.* 152, 706–716.
- [14] Gavrillets, S., Li, H., Vose, M. D., 2000. Patterns of parapatric speciation. *Evolution* 54, 1126–1134.
- [15] Gavrillets, S., Vose, A., 2005. Dynamic patterns of adaptive radiation. *Proc. Natl. Acad. Sci. USA* 102, 18040–18045.
- [16] Getz, W. M., 1984. Population dynamics: A *per capita* resource approach. *J. theor. Biol.* 108, 623–643.
- [17] Hall, M., Christensen, K., di Collobiano, S. A., Jensen, H. J., 2002. Time-dependent extinction rate and species abundance in a tangled-nature model of biological evolution. *Phys. Rev. E* 66, 011904.
- [18] Kauffman, S. A., 1993. The origins of order. Self-organization and selection in evolution. Oxford University Press, Oxford.
- [19] Kauffman, S. A., Johnsen, S., 1991. Coevolution to the edge of chaos: Coupled fitness landscapes, poised states, and coevolutionary avalanches. *J. theor. Biol.* 149, 467–505.
- [20] Krebs, C. J., 1989. *Ecological Methodology*. Harper & Row, New York, Chap. 10.
- [21] Krebs, C. J., 2001. *Ecology. The Experimental Analysis of Distribution and Abundance*. Fifth Edition. Benjamin Cummings, San Francisco.
- [22] Kuang, Y., 2002. Basic properties of mathematical population models. *J. Biomath.* 17, 129–142.
- [23] Martinez, N. D., Williams, R. J., Dunne, J. A., 2006. Diversity, complexity, and persistence in large model ecosystems. In: Pasqual, M., Dunne, J. A. (Eds.), *Ecological Networks: Linking structure to dynamics in food webs*. Oxford University Press, Oxford, pp. 163–185.
- [24] Murray, J. D., 1989. *Mathematical Biology*. Springer-Verlag, Berlin.

- [25] Namba, T., Tanabe, K., Maeda, N., 2008. Omnivory and stability of food webs. *Ecol. Complex.* 5, 73–85.
- [26] Newman, M. E. J., 1996. Self-organized criticality, evolution and the fossil extinction record. *Proc. R. Soc. Lond. B* 263, 1605–1610.
- [27] Newman, M. E. J., Palmer, R. G., 2003. *Modeling Extinction*. Oxford University Press, Oxford.
- [28] Nunes Amaral, L. A., Meyer, M., 1999. Environmental changes, coextinction, and patterns in the fossil record. *Phys. Rev. Lett.* 82, 652–655.
- [29] Procaccia, I., Schuster, H., 1983. Functional renormalization-group study of universal $1/f$ noise. *Phys. Rev. A* 28, 1210–1212.
- [30] Qin, S.-M., Chen, Y., Zhang, P., 2007. Network growth approach to macroevolution. *New J. Phys.* 9, 220.
- [31] Quince, C., Higgs, P. G., McKane, A., 2005. Deleting species from model food webs. *Oikos* 110, 283–296.
- [32] Quince, C., Higgs, P. G., McKane, A., 2005. Topological structure and interaction strengths in model food webs. *Ecol. Modell.* 187, 389–412.
- [33] Resit, H., Arditi, R., Ginzburg, L. R., 1995. Ratio-dependent predation: An abstraction that works. *Ecology* 76, 995–1004.
- [34] Rikvold, P. A., 2005. Fluctuations in models of biological macroevolution. In: Kish, L. B., Lindenberg, K., Gingl, Z. (Eds.), *Noise in Complex Systems and Stochastic Dynamics III*. SPIE, The International Society for Optical Engineering, Bellingham, WA, pp. 148–155, e-print arXiv:q-bio.PE/0502046.
- [35] Rikvold, P. A., 2007. Self-optimization, community stability, and fluctuations in two individual-based models of biological coevolution. *J. Math. Biol.* 55, 653–677.
- [36] Rikvold, P. A., 2009. Degree correlations in a dynamically generated model food web. In: Landau, D. L., Lewis, S. P., Schüttler, H.-B. (Eds.), *Computer Simulation Studies in Condensed Matter Physics XXII*, *Physics Procedia*, in press.
- [37] Rikvold, P. A., Sevim, V., 2007. Individual-based predator-prey model for biological coevolution: Fluctuations, stability, and community structure. *Phys. Rev. E* 75, 051920.
- [38] Rikvold, P. A., Zia, R. K. P., 2003. Punctuated equilibria and $1/f$ noise in a biological coevolution model with individual-based dynamics. *Phys. Rev. E* 68, 031913.
- [39] Rossberg, A. G., Matsuda, H., Amemiya, T., Itoh, K., 2005. An explanatory model for food-web structure and evolution. *Ecol. Complex.* 2, 312–321.
- [40] Rossberg, A. G., Matsuda, H., Amemiya, T., Itoh, K., 2006. Food webs: Experts consuming families of experts. *J. theor. Biol.* 241, 552–563.
- [41] Sevim, V., Rikvold, P. A., 2005. Effects of correlated interactions in a biological coevolution model with individual-based dynamics. *J. Phys. A* 38, 9475–9489.
- [42] Skalski, G. T., Gilliam, J. F., 2001. Functional responses with predator interference: Viable alternatives to Holling type II model. *Ecology* 82, 3083–3092.
- [43] Solé, R. V., Bascompte, J., 1996. Are critical phenomena relevant to large-scale evolution? *Proc. R. Soc. Lond. B* 263, 161–168.
- [44] Thompson, J. N., 1998. Rapid evolution as an ecological process. *Trends Ecol. Evol.* 13, 329–332.
- [45] Thompson, J. N., 1999. The evolution of species interactions. *Science* 284, 2116–2118.
- [46] Verhulst, P. F., 1838. Notice sur la loi que la population suit dans son accroissement. *Corres. Math. et Physique* 10, 113–121.

- [47] Yoshida, K., 2008. The relationship between the duration of food web evolution and the vulnerability to biological invasion. *Ecol. Complex.* 5, 86–98.
- [48] Yoshida, T., Jones, L. E., Ellner, S. P., Fussmann, G. F., Hairston, N. G., 2003. Rapid evolution drives ecological dynamics in a predator-prey system. *Nature* 424, 303–306.
- [49] Zia, R. K. P., Rikvold, P. A., 2004. Fluctuations and correlations in an individual-based model of biological coevolution. *J. Phys. A* 37, 5135–5155.
- [50] The PSDs were calculated by obtaining the averages over octaves in frequency of the periodograms (squared Fourier transforms) of the time series, and then averaging these over the independent simulation runs. The error bars are standard errors, based on the spread between runs.